

**A STUDY OF SPATIAL CELL REPRESENTATIONS IN
COMPLEX ENVIRONMENT USING AN
OSCILLATORY NETWORK**

A Project Report

submitted by

C YASHASVI NIKHIL

in partial fulfilment of the requirements

for the award of the degree of

BACHELOR OF TECHNOLOGY &

MASTER OF TECHNOLOGY



**DEPARTMENT OF ELECTRICAL ENGINEERING
INDIAN INSTITUTE OF TECHNOLOGY, MADRAS.**

MAY 2019

THESIS CERTIFICATE

This is to certify that the thesis titled **A STUDY OF SPATIAL CELL REPRESENTATIONS IN COMPLEX ENVIRONMENT USING AN OSCILLATORY NETWORK**, submitted by **C YASHASVI NIKHIL**, (EE14B079) to the Indian Institute of Technology, Madras, for the award of the degree of **Dual Degree(B.Tech and M.Tech)**, is a bona fide record of the research work done by him under our supervision. The contents of this thesis, in full or in parts, have not been submitted to any other Institute or University for the award of any degree or diploma.

Dr. V Srinivasa Chakravarthy

Research Guide

Professor

Dept. of Biotechnology

IIT-Madras, 600 036

Place: Chennai

Dr. S Umesh

Research Co-Guide

Professor

Dept. of Electrical Engginering

IIT-Madras, 600 036

Date: May 2019

ACKNOWLEDGEMENTS

This thesis becomes a reality with the kind support and help of many individuals. I would like to extend my sincere thanks to all of them.

Foremost, I would like to thank my research advisor **Dr. V Srinivasa Chakravarthy**. The door to Professor office was always open whenever I ran into a trouble spot or had a question about my research or writing. He consistently allowed this thesis to be my own work but steered me in the right the direction whenever he thought I needed it.

I would like to acknowledge **Dr. S Umesh** as the second guide of this thesis, and I am gratefully indebted to him for his very valuable comments on this thesis.

I would also like to thank my labmate **Miss Samyukta Jayakumar** for all the help and guidance that she has provided.

Finally, I must express my very profound gratitude to my parents for providing me with unfailing support and continuous encouragement throughout my years of study and through the process of researching and writing this thesis. This accomplishment would not have been possible without them. Thank you.

TABLE OF CONTENTS

ACKNOWLEDGEMENTS	i
LIST OF FIGURES	iv
ABBREVIATIONS	v
1 INTRODUCTION	1
1.1 A Basic Insight Into The Thesis	1
1.2 Spatial Cells	2
2 LITERATURE REVIEW	5
2.1 Introduction	5
2.2 Background	6
2.3 Methods	7
2.4 VELOCITY DRIVEN OSCILLATORY NETWORK	8
2.4.1 Head direction layer	8
2.4.2 Path integration layer	9
2.4.3 Spatial cell layer	9
2.4.4 LATERAL ANTI HEBBIAN NETWORK (LAHN)	10
2.4.5 PREVIOUS WORK	12
3 EXPERIMENTAL DETAILS	13
3.1 METHODOLOGY	13
3.2 Boundary generation	13
3.3 Trajectory Generation	14
3.4 ALL CELL FIRING FIELDS:	15
3.5 Multi Layered Perceptron	17

4	Results And Future work	18
4.1	2 Compartment	18
4.1.1	Trajectory generation	18
4.1.2	LAHN 1 st Layer	19
4.1.3	LAHN 2 nd Layer	19
4.1.4	LAHN 3 rd Layer	20
4.1.5	MLP	21
4.2	Interpreting the Results	22
4.3	Future works	22
4.3.1	2 Compartments 4 Rooms	23
	REFERENCES	23

LIST OF FIGURES

1.1	Anatomy of hippocampal formation A, anterior; D, dorsal; P, posterior; V, ventral	3
1.2	a Spatial firing pattern of a grid cell from layer II of the rat medial entorhinal cortex (MEC). The grey trace shows the trajectory of a foraging rat in a 2.2m wide square enclosure. The locations at which the grid cell spikes are superimposed on the trajectory are shown in black. Each black dot corresponds to one spike. Note the periodic hexagonal pattern of the firing fields of the grid cell. b Cartoons of firing patterns of pairs of grid cells (shown in blue and green), illustrating the differences between grid scale, grid orientation and grid phase. Lines in left and middle panels indicate two axes of the grid pattern (which define grid orientation); crosses in the panel on the right indicate grid phase (xy location of grid fields).	4
2.1	The network architecture of VDON including the head direction layer, followed by path integration and finally performing principal component analysis for the evolution of different spatial cells. (Soman 2018)	8
2.2	A sample LAHN. White circles - Hebbian connections. Black circles - anti Hebbian	10
2.3	Grid Cell Firings	12
3.1	2 Compartment Boundary	13
3.2	A set of four subfigures.	14
4.1	2 Compartment Trajectory	18
4.2	All cell firing of LAHN 1 st Layer	19
4.3	All cell firing of LAHN 2 nd Layer	20
4.4	All cell firing of LAHN 3 rd Layer	20
4.5	Classification accuracy vs LAHN layers	21
4.6	Trajectory of 2 Compartments 4 Rooms	23
4.7	All cell firing of LAHN 1 st Layer	24
4.8	All cell firing of LAHN 2 nd Layer	24
4.9	All cell firing of LAHN 3 rd Layer	24

ABBREVIATIONS

PI	Path Integration
MEC	Medial Entorhinal Cortex (
SOM	Self Organising Maps
SI	Sensory Integration
LAHN	Lateral Anti-HebbianNetwork
PCA	Principal Component Analysis.
VDON	Velocity Driven Oscillatory Network
OI	Oscillatory Interference
MPO	Membrane Potential Oscillations
LDON	Locomotion Driven Oscillatory Network
VCO	velocity-controlled oscillators
PCA	Principal Component Analysis

CHAPTER 1

INTRODUCTION

1.1 A Basic Insight Into The Thesis

Navigating the environment is an essential part of an animal's survival and accurately estimating its location in the environment is central to this process. The animal uses sensory cues like vision and proprioception (feedback from movement of limbs) to both familiarize itself with the environment and locate itself in it. When experiments were carried out on animals to investigate the neural architecture responsible for this, researchers found a hierarchy of neurons in the Hippocampus region of the brain that seemed to respond to the animal's position, speed and direction.

Further experiments done on animals navigating simple mazes revealed the way the neurons in this hierarchical order are connected. Inputs from visual and proprioceptive neurons feed into sets of neurons called Self Organising Maps (SOMs) which act as encoders to map the input onto a finite set of values. These two types of encoded inputs are then combined in the Sensory Integration (SI) layer using a weighted average which depends on the reliability of incoming information. If there is enough light for reliable visual information, the visual SOM's value will dominate, and vice-versa. At this point, the information in the SI layer's neurons have information on the direction and velocity of the animal (Soman et al. [4]).

The SI layer feeds into the Path Integration (PI) layer via one-to-one connections. As the name suggests, these neurons integrate the incoming velocity information, encoded in

the form of phase difference w.r.t theta oscillations (constant, low frequency oscillations independent of Hippocampus). Finally, the PI layer feeds into a Lateral Anti-Hebbian Network (LAHN) of neurons in a fully-connected fashion. These neurons encode the incoming information in a manner similar to Principal Component Analysis. Ultimately, the LAHN neurons help the animal locate itself as these neurons fire only when the animal is in certain locations in the environment i.e. the firing patterns have relevant spatial information (Soman et al. [4]). These "spatial cells" are the focus of this study.

Study of the firing patterns of these LAHN neurons in different environments can help us better understand the way in which animals navigate their environments. This could ultimately help us improve artificial techniques of navigation in closed, small environments where classical techniques like GPS are not feasible.

1.2 Spatial Cells

The nervous system has evolved to enable adaptive decision making and behaviour in response to changes in the internal and external environment. To permit adaptive responses, nervous systems recreate properties of the internal or external world in activity patterns that are referred to as neural representations. Representations can be thought of as dynamic clusters of cells, the activity patterns of which correlate with features of the outside world. By recreating the environment in a language that is suitable for brain computation, representations are thought to mediate the selection of appropriate action in response to stimulus configurations in the animal's environment.

The medial entorhinal cortex (MEC) and the hippocampus are a part of the brain's neural map of external space. Multiple functional cell types contribute to this representation. The first spatial cell type to be discovered was the place cell. Place cells are hippocampal

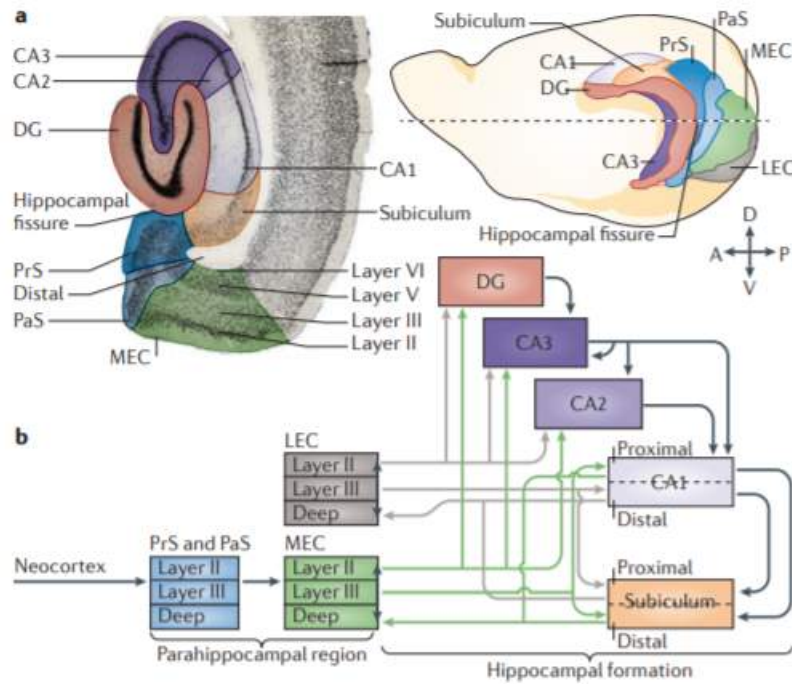


Figure 1.1: Anatomy of hippocampal formation A, anterior; D, dorsal; P, posterior; V, ventral

cells that fire selectively when animals are at certain locations in the environment. The description of place cells in the 1970s was followed, more than 30 years later, by the discovery of grid cells, one synapse upstream of place cells, in the MEC. Grid cells are place-selective cells that fire at multiple discrete and regularly spaced locations. These firing locations form a hexagonal pattern that tiles the entire space that is available to the animal (Figure 1.3a). Whereas ensembles of place cells change unpredictably from one environment to the next, the positional relationship between grid cells is maintained, reflecting the structure of space independently of the contextual details of individual environments. The rigid structure of the grid map, along with its spatial periodicity, points to grid cells as a part of the brain's metric for local space. Place cells and grid cells were discovered in rats, but similar cells have subsequently been reported in mice, bats, monkeys and humans, although the bulk of research on entorhinal hippocampal spatial representation is still carried out using rodents. The strong correspondence in each species between

entorhinal hippocampal firing patterns and a measurable property of the external world the location of the animal makes the spatial representation circuit a powerful experimental model system for understanding neural computation at the highest levels of the association cortices, many synapses away from sensory receptors and motor outputs. The defining

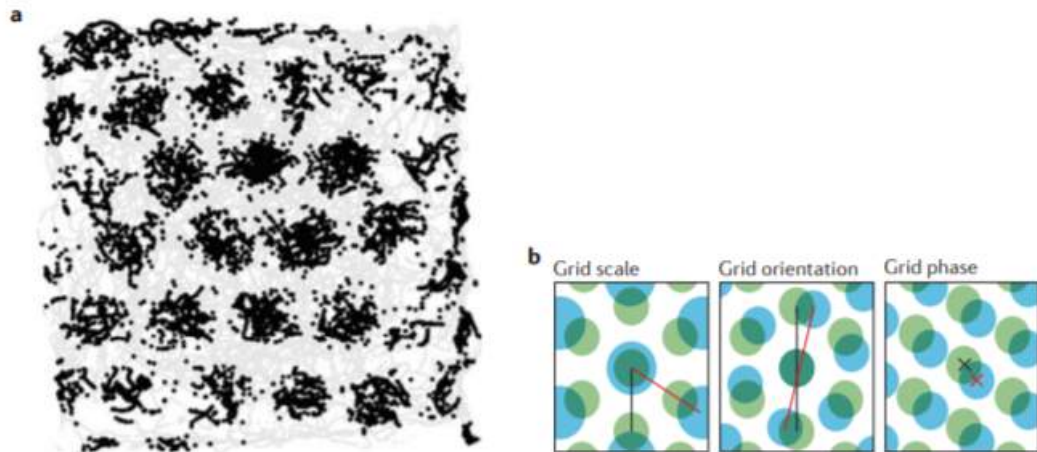


Figure 1.2: a | Spatial firing pattern of a grid cell from layer II of the rat medial entorhinal cortex (MEC). The grey trace shows the trajectory of a foraging rat in a 2.2m wide square enclosure. The locations at which the grid cell spikes are superimposed on the trajectory are shown in black. Each black dot corresponds to one spike. Note the periodic hexagonal pattern of the firing fields of the grid cell. b | Cartoons of firing patterns of pairs of grid cells (shown in blue and green), illustrating the differences between grid scale, grid orientation and grid phase. Lines in left and middle panels indicate two axes of the grid pattern (which define grid orientation); crosses in the panel on the right indicate grid phase (xy location of grid fields).

feature of grid cells is their hexagonal firing structure. However, grid cells differ in grid spacing (the distance between grid fields), grid orientation (the rotation of grid axes) and grid phase (the xy locations of firing vertices).

CHAPTER 2

LITERATURE REVIEW

2.1 Introduction

Spatial cells in the hippocampal complex play a pivotal role in the navigation of an animal. Exact neural principles behind these spatial cell responses have not been completely unraveled yet. Here we look at two models for spatial cells, namely the Velocity Driven Oscillatory Network (VDON) and Locomotor Driven Oscillatory Network. Both models have basically three stages in common such as direction encoding stage, path integration (PI) stage, and a stage of unsupervised learning of PI values. In the first model, the following three stages are implemented: head direction layer, frequency modulation by a layer of oscillatory neurons, and an unsupervised stage that extracts the principal components from the oscillator outputs. In the second model, a refined version of the first model, the stages are extraction of velocity representation from the locomotor input, frequency modulation by a layer of oscillators, and two cascaded unsupervised stages consisting of the lateral anti-hebbian network. The principal component stage of VDON exhibits grid cell-like spatially periodic responses including hexagonal firing fields. Locomotor Driven Oscillatory Network shows the emergence of spatially periodic grid cells and periodically active border-like cells in its lower layer; place cell responses are found in its higher layer. This model shows the inheritance of phase precession from grid cell to place cell in both one and two-dimensional spaces. It also shows a novel result on the influence of locomotion rhythms on the grid cell activity. The study thus presents a comprehensive, unifying hierarchical model for hippocampal spatial cells.

2.2 Background

Place cells fire whenever the animal visits a certain location in the ambient space. This discovery had led to subsequent discovery of a larger class of hippocampal cells that represent space, collectively known as the 'spatial cells' (O'Keefe & Dostrovsky, 1971; Taube et al., 1990a,b; Hafting et al., 2005; Solstad et al., 2008). Taube et al. (1990a) discovered a group of neurons from the postsubiculum region that fired only when the animal's head was in a particular direction in the horizontal plane (yaw plane) (Taube et al., 1990a,b). These so-called head direction (HD) cells are thought to constitute an 'internal compass' that gives a sense of direction to the animal (Valerio & Taube, 2012). Hafting et al. (2005) described a group of neurons in medial entorhinal cortex (MEC) that had a firing field with an astonishingly geometric regularity: multiple firing fields of a single neuron of this type roughly formed the vertices of a hexagon. As the firing field tessellated the ambient space into a hexagonal grid-like pattern, they were named the grid cells.

Efforts have been made to gain insight into spatial cell responses using computational models. With regard to grid cell modeling, existing models fall into two broad categories: oscillatory interference (OI) models and attractor network models. In the OI model, originally proposed for place cells by O'Keefe & Recce (1993), two subthreshold membrane potential oscillations (MPO), one with constant frequency and the other with variable frequency which in turn was a function of the velocity of the animal, were considered. The interference between them resulted in patterns that gave rise to spiking over spatially periodic locations. This was extended to explain the grid field formation on a two-dimensional space (Burgess et al., 2007). To account for the triangular/hexagonal grid formation, the directional modulation of the variable oscillations was assumed to differ by multiples of 60° . Many variations of this model have been proposed which use coupled noisy spiking neurons instead of sinusoidal oscillators as VCOs, to generate the grid firing fields, and

these models were also validated using experimental data (Blair et al., 2008; Hasselmo, 2008; Zilli Hasselmo, 2010). The merit of interference models is that the resetting of path integration (PI) takes place naturally because of the inherent periodicity in the oscillations rather than using hard resets like modulo functions (Gaussier et al., 2007). These models also successfully explained many grid cell data and also came up with predictions on grid-scale variation. However, the drawback in these models was the assumption of 60° constraints on the direction modulation of the oscillators. There were modeling efforts to circumvent the aforementioned constraint problem such that 60° phase separation was formed through a self-organizing process (Mhatre et al., 2012). However, these models had a predisposition to explain specifically the grid field formation and could not explain the principle behind the formation of other spatial cells.

2.3 Methods

In this section, we present two models of spatial cells: Velocity Driven Oscillatory Network (VDON) and Locomotion Driven Oscillatory Network (LDON). Since VDON is more transparent due to its simplicity, it reveals a key insight in our modeling approach. This explains how the periodicity arises in the spatial cell responses though there is no periodicity in the input, nor is there any special symmetry in the network architecture. Both models have three common architectural elements viz. Direction encoding layer / Head Direction (HD) layer, Path Integration (PI) layer, and layer of unsupervised neural network. Both models do not use any special symmetry in the HD layer. The HD layer responses are integrated in the next layer known as the PI layer. The PI layer in turn projects, via trainable connections, to another layer where a variety of spatial cells, particularly a variety of grid cells, naturally emerge. Albeit VDON and LDON share this architecture, LDON is a biologically plausible extension of VDON. A virtual animal is made to forage

inside a square box of size two units. Trajectories of the animal, that involve an upper limit on curvature, are constructed using a method .In VDON, the virtual animal is represented as a point, and its motion is represented explicitly in terms of speed, s , and direction, θ . In LDON, the virtual animal is represented as a four-legged creature and motion is represented in terms of four locomotor rhythms generated by the legs.

2.4 VELOCITY DRIVEN OSCILLATORY NETWORK

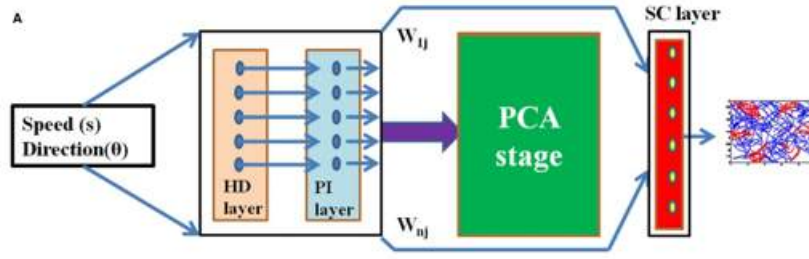


Figure 2.1: The network architecture of VDON including the head direction layer, followed by path integration and finally performing principal component analysis for the evolution of different spatial cells. (Soman 2018)

2.4.1 Head direction layer

Head direction layer is composed of array of neurons each having its own preferred direction. The response of i_{th} HD cell is computed as the projection of the animal's current direction onto the i_{th} preferred direction, given as,

$$HD_i = \cos(\theta - \theta_i)$$

θ is the current heading direction of the animal, and θ_i is the preferred direction of i_{th} HD cell.

2.4.2 Path integration layer

Path integration layer has an array of oscillators with one-to-one connection with the HD layer. To achieve PI, the frequency of the oscillator is modulated by the speed and the HD layer response. Hence, phase of the i_{th} oscillator codes for the position of the animal in that preferred direction. This completes the PI process. Interference model also implemented position encoding using the phase of the velocity-controlled oscillators (VCO) (Burgess et al., 2007). Comparison to interference model is performed in the discussion section in detail. Frequency modulation of i_{th} PI oscillator with a base frequency f_0 is given as

$$PI_i = \sin\left[\int 2\pi(f_0 + \beta s HD_i)\right]$$

where β is the modulation factor, and s is speed of the animal.

State of i_{th} PI neuron, PI_i , is then thresholded by the following rule,

$$PI_i^{Thr} = H(PI_i - \epsilon_{PI}).PI_i$$

where, H is the Heaviside function, and ϵ_{PI} is the threshold value.

2.4.3 Spatial cell layer

Spatial cell layer represents the region of Entorhinal Cortex (EC) to which the PI response vector converges as input (Figure. 2.1). The thresholded PI values are projected via a linear weight stage (WPC) to the SC layer. Weight (WPC) from PI to SC neuron is computed by performing principal component analysis (PCA) over PI^{Thr} . PCA was performed analytically by extracting the top few Eigen vectors (selected based on the Eigen value spectrum) of the covariance matrix of the PI^{Thr} (Karhunen Joutsensalo, 1995). The response of i_{th}

neuron in the SC layer is given as,

$$SC_i = \sum_{j=1}^N H[W_{ij}^{PC} \cdot PI_j^{Thr} - \epsilon_{SC}]$$

where H is Heaviside function, N is the number of PI neurons, and ϵ_{SC} is the threshold value. W_{ij}^{PC} is the weight connection from j_{th} PI neuron to i_{th} SC neuron. Neurons receiving the top few principal components (PC) will be shown to reveal a variety of spatial cell-like responses including grid cells (both hexagonal and square grid cells) and corner cells (whose firing fields are at the corners of the space) as shown in the results section. The emergence of spatially periodic firing field is due to the inherent periodicity in the PC weights. The neurons that receive PCs whose peaks are separated by $\approx 60^\circ$ show hexagonal grid cell-like activity. The current PCA approach has some resemblance to the model of Dordek et al. (2016) which used PCA to produce grid formation from place cell activity.

2.4.4 LATERAL ANTI HEBBIAN NETWORK (LAHN)

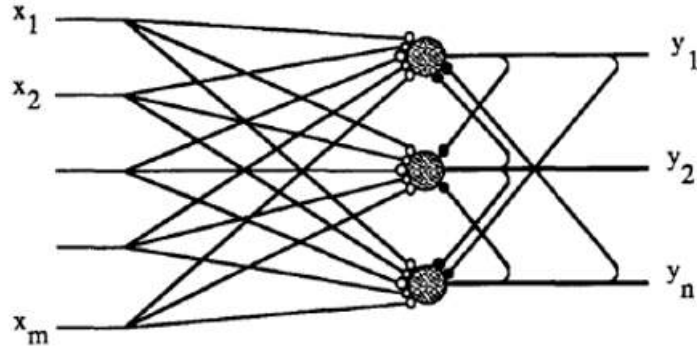


Figure 2.2: A sample LAHN. White circles - Hebbian connections. Black circles - anti Hebbian

The LAHN is a set of neurons connected to each other such that incoming inputs are connected in a Hebbian manner (forward weights) and connections between neurons are connected in an anti-Hebbian manner (lateral weights). The anti-Hebbian connections

act as a decorrelation network, removing correlations between incoming inputs as far as possible (P.Foldiak 1989). As a result, the LAHN acts as an effective dimensionality reduction network while maintaining maximum mutual information flow between input and output. Similar to PCA, this network projects the input onto a subspace of its largest principal components (dimensions with greatest variance) having least cross-correlation between them.

Training this network happens in an unsupervised manner, using simple localized rules for modification of connection weights. Not only is the training faster this way, it is also biologically more plausible than classical error propagation rules. The network training is said to have converged when the maximum change in weight of a connection (both forward and lateral) is less than a specified threshold

The output of each neuron is as follows:

$$y_i = \sum_{j=1}^m q_{ij}x_j + \sum_{j=1}^n w_{ij}y_j$$

where w_{ij} and q_{ij} are forward and lateral weights respectively. Written in matrix form:

$$Y = QX + WY$$

$$Y = (1 - W)^{-1}QX$$

During training, the rules for modification of these weights are as follows:

$$\Delta w_{ij} = -\alpha y_i y_j$$

$$\Delta q_{ij} = \beta (y_i x_j - q_{ij} y_i^2)$$

where α and β are the learning rates for each connection.

In the full model of the neural architecture, there are two sets of LAHNs - the spatial cell layer $LAHN_{SC}$ and the place cell layer $LAHN_{PC}$, each producing different types of firing fields. The simplified model, on the other hand, has just one layer of LAHN neurons.

2.4.5 PREVIOUS WORK

Previous experiments and model simulations have been done in which the animal is constrained to a 2D plane (rats). The neuron firing fields obtained from the simulations contain a set of points where the neuron fires. This needs to be converted into a 2D map of strength of activation of the neurons at these points. The entire environment is divided into bins and if a point in the firing field exists in that bin, its value is increased. Cell firings are categorized as:

Place cells - These cells only fire when the animal is in the vicinity of a particular point in the environment.

Grid cells - These cells only fire when the animal is on the vertices of a repeating pattern on the environment. These repeating patterns may be overlapping hexagons or squares.

Border cells - These cells only fire when the animal is in the vicinity of a border of the environment.

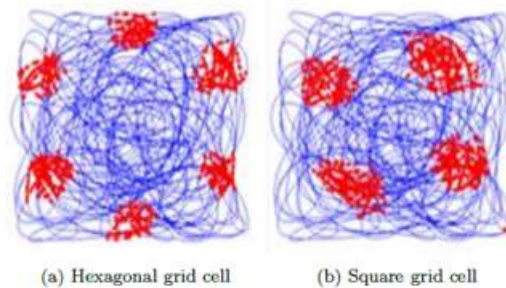


Figure 2.3: Grid Cell Firings

CHAPTER 3

EXPERIMENTAL DETAILS

3.1 METHODOLOGY

We look at the various steps involved in the methodology including a few code showing the parameters involved. The whole methodology can be divided into four broad steps:

1. **Boundary generation:** Building bounding boxes for custom trajectory generation
2. **Trajectory Generation:** Random trajectory generation in the generated bounding box with emphasis to continuity
3. **All cell firing fields:** Finding all neuron findings in L1, L2, L3 layers of LAHN
4. **Multi layered Perceptron:** Use MLP and find percentage of compartment features in firing cell patterns at the end of each layer

3.2 Boundary generation

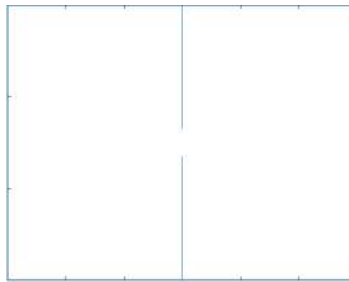


Figure 3.1: 2 Compartment Boundary

We begin the study with generating a two compartment boundary. Initially , we created 2 rooms with a connection in between , this was further modified to 2 compartment rooms to make the analysis simple.

3.3 Trajectory Generation

Generating a trajectory in the above boundary condition is quite tough without considering or putting constraints on entry and exit of the trajectory from a room. So, we put a constraint: when ever there is a room shift in trajectory ,the point has to come to a point close to the opening in the partition between the rooms and then move to next compartment. This process of directing a point towards the junction of the room opening is being done by the model **converge**. This model takes input of the start and end point coordinates and fits in a fine trajectory in between the two points. The trajectory can be tuned based on the requirements to fit in the trajectory based on the need, it can generate trajectory with variable randomness(curves) i.e as shown in Figure 3.2.

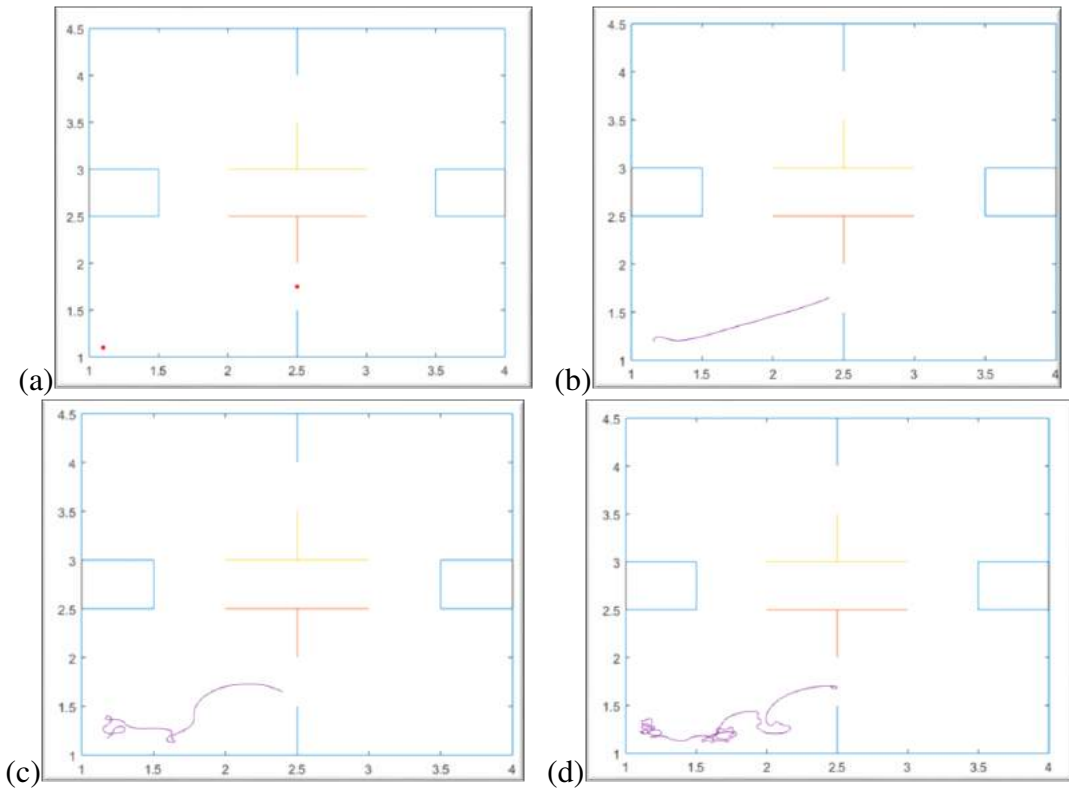


Figure 3.2: Trajectory between 2 points using **converge** method: a) start and end point; b) smooth curveless fit; c) less curves; and d) more curves

This method is used in between the room switches which are scheduled to occur after every 2000 trajectory points.

3.4 ALL CELL FIRING FIELDS:

We generate three data files from the trajectory generation section viz. a coordinates file, head direction file and speed file. These files contain data in matrices enclosing the trajectory coordinates, the angle of the head direction (\hat{y}) and speed of the animal (s). We load this data in our model and feed the values to the HD layer to compute the HD responses.

```
1 %% HD response computing
2 speed = speed';
3 phase1d = zeros(100,1);
4 X=[];
5 trj_hd_resp=[];
6 for ii = 1:size(speed,2)
7     X1 = [cosd(theta_real_deg(1)) sind(theta_real_deg(1))]; X2 = [cosd(
8         theta_real_deg(ii)) sind(theta_real_deg(ii))];
9     s1 = X2(1)*X1(2) - X1(1)*X2(2); %sin(theta1-theta2)
10    s2 = X2(1)*X1(1) + X1(2)*X2(2); %cos(theta1-theta2)
11    X=[s1 s2];
12    y = respsom2dlinear(X,wt2);
13    trj_hd_resp(:, :, ii) = y;
14    ii
15 end
```

Listing 3.1: Computation of HD layer response

We feed the speed values and the HD layer responses to the PI layer.

```
1 %% PI osc
2 X = zeros(100,1); Y = ones(100,1); %Xarr=[]; Yarr=[];
3 dt = 0.01;
4 bf = 6*2*pi;
5 niter = size(trj_hd_resp,3);
6 betaa = 55; t = 0;
```

```

7 Xbg = 1; Ybg = 0;
8 tarr=[];
9 theta=zeros(100,1);
10 for ii = 2:niter
11     ii
12     y = trj_hd_resp(:, :, ii);
13     inpld = reshape(y,100,1);
14     thetadot = bf + betaa*speed(ii)*inpld*10;
15     theta(:, ii)=theta(:, ii-1)+thetadot*dt;
16 end
17 Xarr=cos(theta);
18 PIld=Xarr;

```

Listing 3.2: Oscillatory output from the PI layer

We continue to perform PCA using the LAHN with an output neuron number of 40. The LAHN takes many iterations to converge. Loading the weights, we continue to find the neuron firings in L1 layer of the LAHN.

```

1 %% All cell firing field
2 %load('L1-weights_com2.mat');
3 % figure
4 % foldiak1respmat=[];
5 for ii=1:size(T,1)
6     subplot(5,8,ii); w=T(ii,:);w = w';
7     ot=w'*(PIld); ot=ot';
8     thresh=max(ot)*.75;
9     firr=find(abs(ot)>thresh);
10    foldiak1respmat(ii,:) = ((abs(ot)>thresh).*ot)';
11    firposgrid=pos(firr,:);
12    plot(pos(:,1),pos(:,2));
13    %set(gcf,'units','3,3');

```

```

14     hold on; plot(firposgrid(:,1),firposgrid(:,2),'.r', 'markersize',
15     10);
15 end

```

Listing 3.3: Plotting the neuron firings in the L1 layer of LAHN with a set threshold of 0.75

We continue to perform PCA using LAHN for the second and third layer with an output neuron number of 25 and 9 respectively. The LAHN takes two iterations to converge.

3.5 Multi Layered Perceptron

In the multi-compartment navigation module, an additional layer of LAHN is added in order that compartment specific features are isolated. We generated a two-compartment model where the virtual agent forages one room for a stipulated time after which it enters the other room through the narrow doorway present between the compartments. This is repeated for a time (t) (I.e length of the trajectory) . All three LAHN layers exhibit certain features of both the compartment, hence in order to confirm which layer holds a more room-specific feature, we used a multi-layer perceptron (MLP) to quantify the % of accuracy of classification between the rooms.

CHAPTER 4

Results And Future work

4.1 2 Compartment

4.1.1 Trajectory generation

we chose a random point in the boundary (Figure 3.1) and start random trajectory in that particular compartment. After finishing a fixed number of iterations in one compartment, compartment shift happens with 0.8 probability. To shift compartment we first use the **converge** function to generate a trajectory from the last point of the iteration to the point close to the partition opening. And if there is no compartment shift random trajectory is continued in the same compartment. This is done for 60,000 iterations in total with 2000 number of iterations between each decision taken for compartment shift.

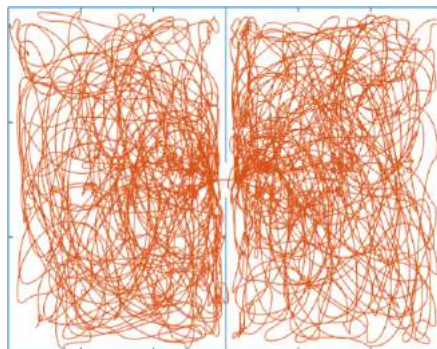


Figure 4.1: 2 Compartment Trajectory

4.1.2 LAHN 1st Layer

Head direction , position and speed data from the Trajectory is feed into the VDON model (HD layer , PI layer and LAHN). Below are the all cell firings after one LAHN layer with threshold set at 0.65.

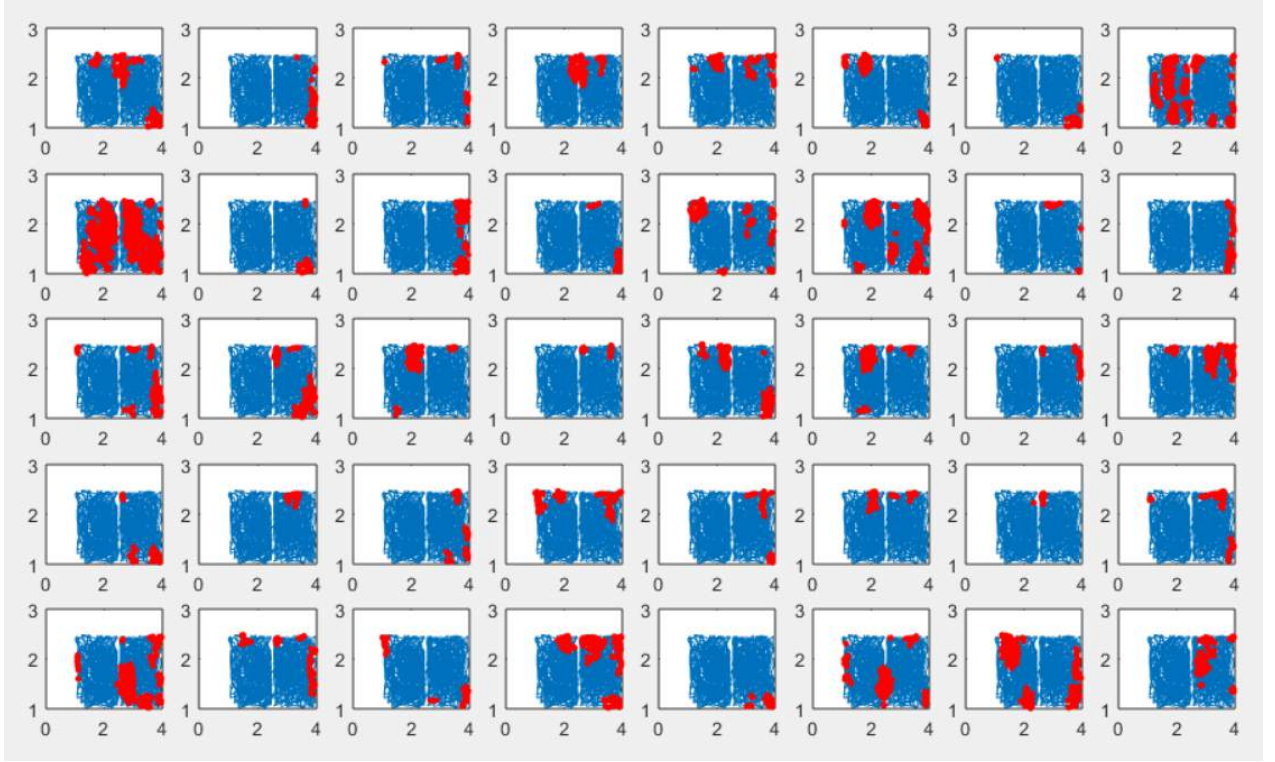


Figure 4.2: All cell firing of LAHN 1st Layer

4.1.3 LAHN 2nd Layer

Foldiak response of the first layer is fed as input into the second layer. Below are the all cell firings after second LAHN layer with threshold set at 0.75.

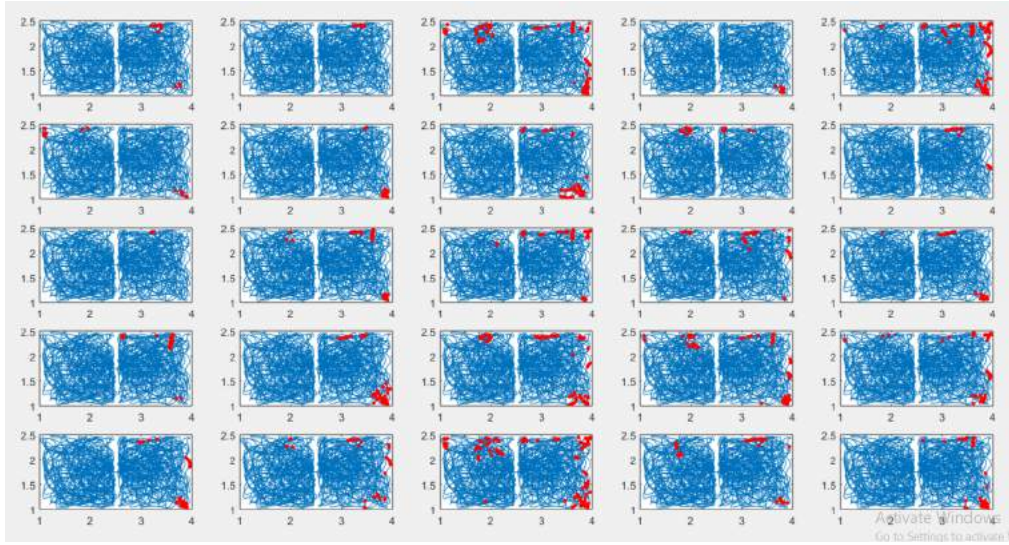


Figure 4.3: All cell firing of LAHN 2nd Layer

4.1.4 LAHN 3rd Layer

same as in 2nd layer, Foldiak response of the second layer is fed as input into the 3rd layer.

Below are the all cell firings after 3rd LAHN layer with threshold set at 0.75.

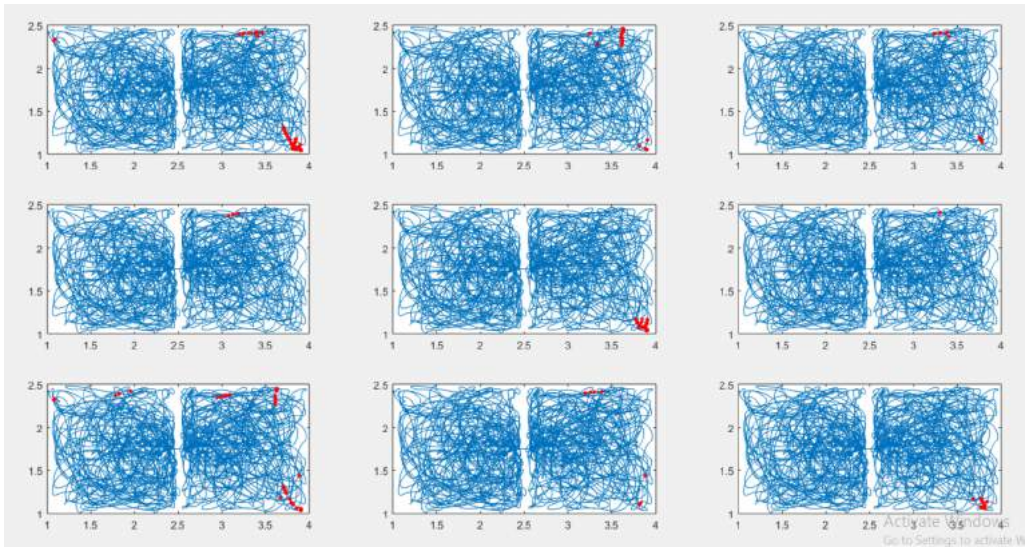


Figure 4.4: All cell firing of LAHN 3rd Layer

4.1.5 MLP

All three LAHN layers exhibit certain features of both the compartment, hence in order to confirm which layer holds a more room-specific feature, we used a multi-layer perceptron (MLP) to quantify the % of accuracy of classification between the rooms.

The graph shows the classification accuracy vs LAHN layers It can be inferred that, layer 3 (LAHN - 3) shows the highest classification accuracy thus concluding that the optimal information about features specific to each compartment is encoded in this layer.

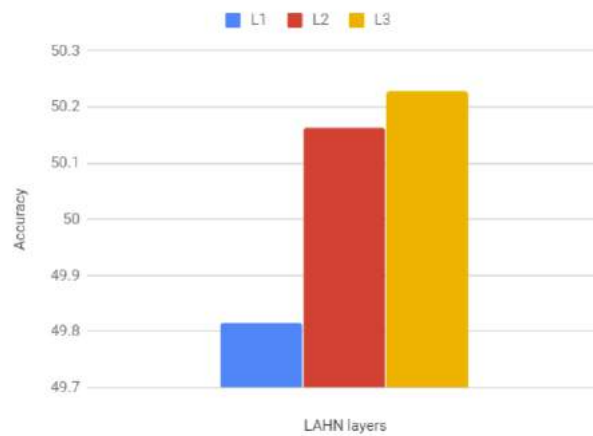


Figure 4.5: Classification accuracy vs LAHN layers

4.2 Interpreting the Results

From all cell firing of first layer, we are able to see neurons which are:

- compartment specific ->also seen in 2nd3rd LAHN layers)
- Firing at corners
- Firing at partition
- Grid cells
- etc..

We need different models for every feature to prove it.

MLP:The key observation is layer 3 (LAHN - 3) shows the highest classification accuracy thus concluding that the optimal information about features specific to each compartment is encoded in this layer. There may be several reasons for this observation:

- **Too few LAHN neurons** Since the environment, and hence the animal's path, is more complex, the limited number of LAHN neurons may be forced to learn simpler representations. Introduction of more LAHN neurons could give the network the ability to learn more complex representations.
- **Consequence of small environment** - The simulation is carried out in a 3x1.5 box with a resolution of 0.1 for the firing rate map. As a result, clustering might not have happened.
- **Local vs Global grid scores** - In the above analysis, very less variation in accuracy is observed. Some previous works have simulated 2D environments with obstacles and concluded that as the size of obstacles increase, the network begins to learn the presence of the separate regions. Some neurons only fire when the animal is in one region, but including more compartments may also increase compartment specific features.

4.3 Future works

2 compartment trajectory is first step in the spatial navigation. This can be extended to many ways for future works. Few of them are:

- Improved feature extraction from the LAHN layer by adding a new dimensionality using visual input
- Adding more rooms and compartments: example of 4 rooms 2 compartment trajectory in next section
- 3D multi-floored trajectory : Adding the floors with more than 2 rooms in each floor and studying the model in 3D environment.
- Adding objects (marker point) to see if it effects the cell firing

4.3.1 2 Compartments 4 Rooms

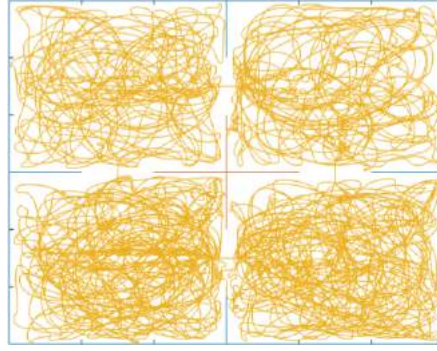


Figure 4.6: Trajectory of 2 Compartments 4 Rooms

This is extension to the 2 compartment problem. In this there are 2 compartments (one above and other below) with 2 rooms each. The compartments are connected such that they can shift to other room in same compartment or to the connecting room of other compartment. The switching between compartments or rooms of same compartment is done based on the probability.

P_{com} – probability of switch between compartments P_r – probability of switch between rooms of same compartment

$$P_{com} + P_r = 1$$

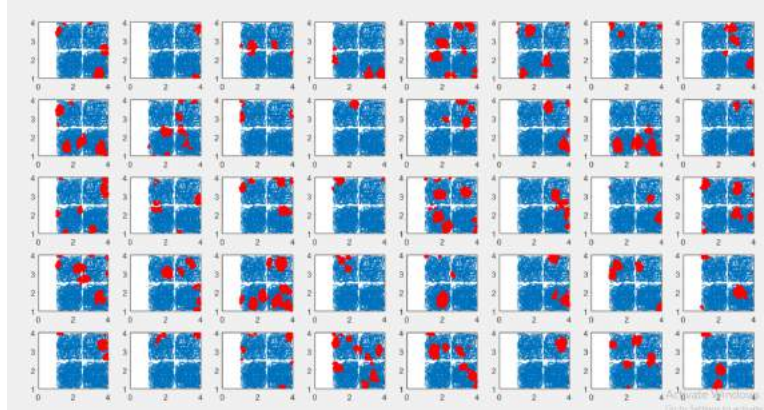


Figure 4.7: All cell firing of LAHN 1st Layer

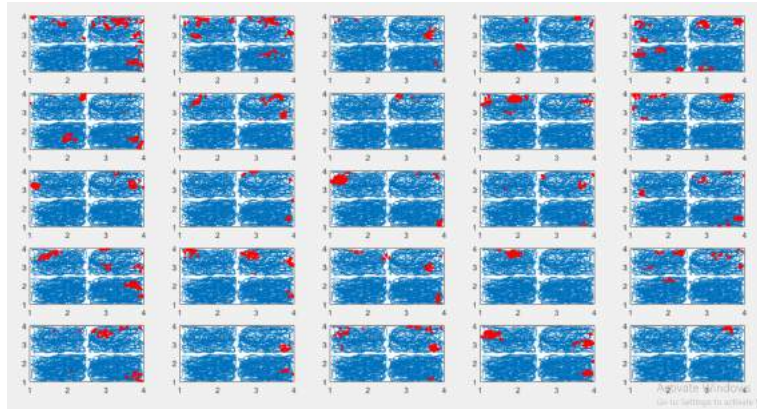


Figure 4.8: All cell firing of LAHN 2nd Layer

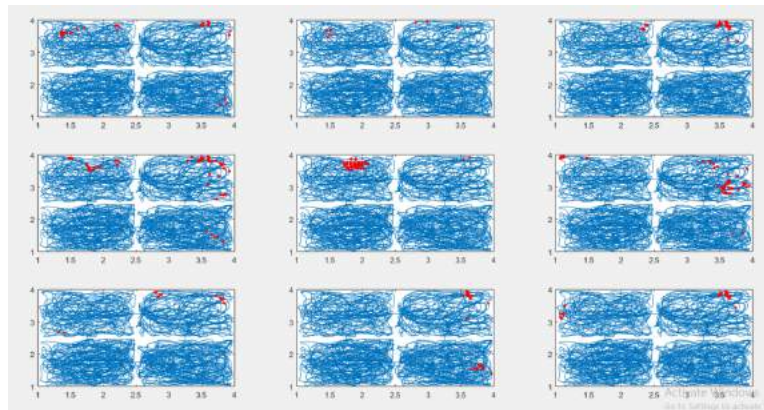


Figure 4.9: All cell firing of LAHN 3rd Layer

REFERENCES

- [1] **K.Soman, V.Muralidharan, S.Chakravarthy.** AN OSCILLATORY NETWORK MODEL OF HEAD DIRECTION, SPATIALLY PERIODIC CELLS AND PLACE CELLS USING LOCOMOTOR INPUTS. 2016.
- [2] **K.Soman, S.Chakravarthy, M.M.Yartsev.** A Hierarchical Anti-Hebbian Network Model for the Formation of Spatial Cells in Three-Dimensional Space. 2018.
- [3] **K.Soman, V.Muralidharan, S.Chakravarthy.** A Model of Multisensory Integration and its Influence on Hippocampal Spatial Cell Responses. IEEE 2017.
- [4] **K.Soman, V.Muralidharan, S.Chakravarthy.** A unified hierarchical oscillatory network model of head direction cells, spatially periodic cells, and place cells. European Journal of Neuroscience 2018
- [5] **P. Foldiak.** Adaptive Network for optimal Linear Feature Extraction. 1989.
- [6] **Jayakumar, S., Narayanamurthy, R., Ramesh, R., Soman, K., Muralidharan, V., Chakravarthy, V. S.** (2018). Modeling the Effect of Environmental Geometries on Grid Cell Representations. *Frontiers in neural circuits*, 12, 120.
- [7] **Fyhn, M., Hafting, T., Witter, M. P., Moser, E. I., Moser, M. B.** (2008). Grid cells in mice. *Hippocampus*, 18(12), 1230-1238.
- [8] **Miller, Jonathan F., Markus Neufang, Alec Solway, Armin Brandt, Michael Trippel, Irina Mader, Stefan Hefft et al.** "Neural activity in human hippocampal formation

reveals the spatial context of retrieved memories." *Science* 342, no. 6162 (2013): 1111-1114.

- [9] Moser, Edvard I., and May-Britt Moser. "Grid cells and neural coding in high-end cortices." *Neuron* 80, no. 3 (2013): 765-774.